THE JOURNAL OF BIOLOGICAL CHEMISTRY VOL. 285, NO. 1, pp. 655–666, January 1, 2010

IcmF Is a Fusion between the Radical B_{12} Enzyme Isobutyryl-CoA Mutase and Its G-protein Chaperone*[S]

Received for publication, September 3, 2009, and in revised form, October 25, 2009 Published, JBC Papers in Press, October 28, 2009, DOI 10.1074/jbc.M109.062182

Valentin Cracan, Dominique Padovani[1], and Ruma Banerjee[2]

From the Department of Biological Chemistry, University of Michigan, Ann Arbor, Michigan 48109

Coenzyme B_{12} is used by two highly similar radical enzymes, which catalyze carbon skeleton rearrangements, methylmalonyl-CoA mutase and isobutyryl-CoA mutase (ICM). ICM catalyzes the reversible interconversion of isobutyryl-CoA and *n*-butyryl-CoA and exists as a heterotetramer. In this study, we have identified >70 bacterial proteins, which represent fusions between the subunits of ICM and a P-loop GTPase and are currently misannotated as methylmalonyl-CoA mutases. We designate this fusion protein as IcmF (isobutyryl-CoA mutase fused). All IcmFs are composed of the following three domains: the N-terminal 5′-deoxyadenosylcobalamin binding region that is homologous to the small subunit of ICM (IcmB), a middle P-loop GTPase domain, and a C-terminal part that is homologous to the large subunit of ICM (IcmA). The P-loop GTPase domain has very high sequence similarity to the *Methylobacterium extorquens* MeaB, which is a chaperone for methylmalonyl-CoA mutase. We have demonstrated that IcmF is an active ICM by cloning, expressing, and purifying the IcmFs from *Geobacillus kaustophilus*, *Nocardia farcinica,* and *Burkholderia xenovorans*. This finding expands the known distribution of ICM activity well beyond the genus *Streptomyces,* where it is involved in polyketides biosynthesis, and suggests a role for this enzyme in novel bacterial pathways for amino acid degradation, myxalamid biosynthesis, and acetyl-CoA assimilation.

Isobutyryl-CoA mutase (ICM)[3] (EC 5.4.99.13) is a coenzyme B_{12} (or 5′-deoxyadenosylcobalamin (AdoCbl))-dependent enzyme, which catalyzes the rearrangement of isobutyryl-CoA to *n*-butyryl-CoA (1–3). This reaction is very similar to that catalyzed by methylmalonyl-CoA mutase (MCM), which is better studied and more widely distributed in nature (4). In both reactions, carbon skeleton rearrangements take place where the carbonyl-CoA substituent and a hydrogen atom on neighboring carbon atoms exchange positions (Fig. 1) (2, 3). The genes encoding ICM were first cloned and sequenced from the Gram-positive, filamentous soil bacterium *Streptomyces cinnamonensis.* ICM is an $\alpha_2\beta_2$ heterotetramer composed of two large subunits (IcmA) of 62.5 kDa and two small subunits (IcmB) of 14.3 kDa. The genes encoding the subunits of MCM, an $\alpha\beta$ heterodimer in some bacteria, are usually located in a single operon (Fig. 2). In contrast, the *icmA* and *icmB* genes are distant from each other in the genome of *S. cinnamonensis* (2).

The sequence of IcmA is very similar to the sequences of the large subunit of MCM, with the exception of the AdoCbl binding region, which is missing. Thus, IcmA lacks a C-terminal AdoCbl binding domain containing the signature D*X*H*XX*G motif that is present instead in the small IcmB subunit, which binds the cofactor (5). In this respect, ICM resembles some other AdoCbl-dependent mutases that exhibit a similar organization. For example, glutamate mutase is also composed of two subunits of very different sizes as follows: the large subunit MutE, which binds substrate, and the small subunit MutS, which binds AdoCbl (6).

The ICM-catalyzed reaction plays an important role in polyketide biosynthesis in *Streptomyces*. In studies with ^{13}C-labeled isobutyrate, it was shown that this compound efficiently incorporates into monensin A tylosin and leucomycin at positions derived from *n*-butyrate (1). Although ICM was believed to have a rather limited distribution, its close sequence relative, MCM, is present in organisms ranging from bacteria to man (7).

A G-protein chaperone, MeaB, shows strong operonic association with MCM, and mutations in the human ortholog, the product of the *cbl*A locus, result in methylmalonic aciduria due to dysfunctional MCM activity (8). MeaB from *Methylobacterium extorquens* has been characterized most extensively and is a P-loop GTPase (9, 10). Other members of this subfamily include HypB, UreG, and CooC, which are important in the assembly of the following metalloenzymes: nickel hydrogenases (11), urease (12), and CO dehydrogenase (13), respectively. MeaB has been proposed to function in the GTP-dependent assembly of holo-MCM and shown to protect the radical intermediates formed during MCM catalysis from oxidative interception (14). MCM, in turn, influences the GTPase activity of MeaB increasing it by >100-fold. Hence, MCM exhibits GTPase-activating protein activity for MeaB (14, 15). In addition, MCM modulates the affinity of MeaB for nucleotides. The crystal structure of MeaB in the presence of GDP has been solved and confirms that it is a member of the G3E family of GTPases but differs from other family members in possessing N- and C-terminal extensions of unknown function (9). Structural insights into the interaction between MeaB and MCM are lacking.

* This work was supported, in whole or in part, by National Institutes of Health Grant DK45776.

[S] The on-line version of this article (available at http://www.jbc.org) contains supplemental Tables S1–S2 and Figs. S1–S3.

[1] Present address: Laboratoire d'Enzymologie et Biochimie Structurales, UPR3082 CNRS, 91198 Gif/Yvette, France.

[2] To whom correspondence should be addressed: 3220B MSRB III, 1150 W. Medical Center Dr., Ann Arbor, MI 48109-5606. Tel.: 734-615-5238; E-mail: rbanerje@umich.edu.

[3] The abbreviations used are: ICM, isobutyryl-CoA mutase; MCM, methylmalonyl-CoA mutase; GMPPNP, guanosine-5′-[(β,γ)-imido]triphosphate; TCEP, tris(2-carboxyethyl)phosphine hydrochloride; AdoCbl, 5′-deoxyadenosylcobalamin; BDH, butyryl-CoA dehydrogenase; LIC, ligase-independent cloning.

In this study, we show that in >70 bacteria ICM is fused to a P-loop GTPase, which is a paralog of MeaB. This fusion protein that we have named IcmF (for ICM-fused) is described as a putative MCM-like protein in the data bases. The misannotation has led to the ascription of this gene product as representing a fusion between MCM and MeaB (16) and to its function in pathways that are unlikely to be correct (17). Using bioinformatics and biochemical approaches, we demonstrate that IcmF is an ICM with ICM and GTPase activities. IcmF represents an important paradigm for elucidating the cross-talk between a mutase and its auxiliary protein during the catalytic cycle.

EXPERIMENTAL PROCEDURES

Materials

AdoCbl, GTP, GMPPNP, GDP, isobutyryl-CoA, and *n*-butyryl-CoA were purchased from Sigma. Tris(2-carboxyethyl)phosphine hydrochloride (TCEP) was purchased from Pierce. Butyric, isobutyric, and valeric acids were purchased from Fluka. [^{14}C]CH_3-malonyl-CoA (56 Ci/mol) was purchased from PerkinElmer Life Sciences. A construct harboring butyryl-CoA dehydrogenase from *Megasphaera elsdenii* was a generous gift from Donald Becker (University of Nebraska, Lincoln).

Cloning and Expression of IcmF

The *icmF* gene from three organisms was cloned into the pET-30 Ek/LIC expression vector (Novagen, CA). The genomic DNA of *Geobacillus kaustophilus* and *Burkholderia xenovorans* (formerly known as *Burkholderia fungorum*) were generous gifts from Hideto Takami (Japan Agency for Marine-Earth Science and Technology, Kanagawa, Japan) (18). The genomic DNA clone KNL023_G20 in the pTS1 plasmid containing the *Nocardia farcinica icmF* gene was obtained from Jun Ishikawa (National Institute of Infectious Diseases, Tokyo, Japan) (19).

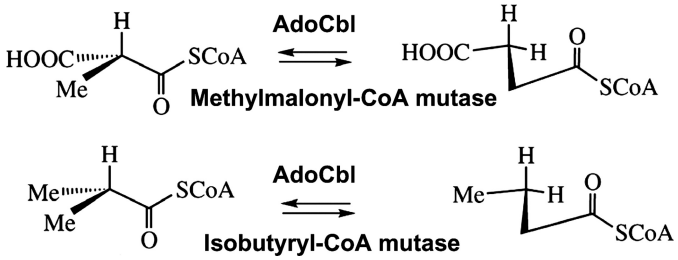

FIGURE 1. **Reactions catalyzed by MCM and ICM.**

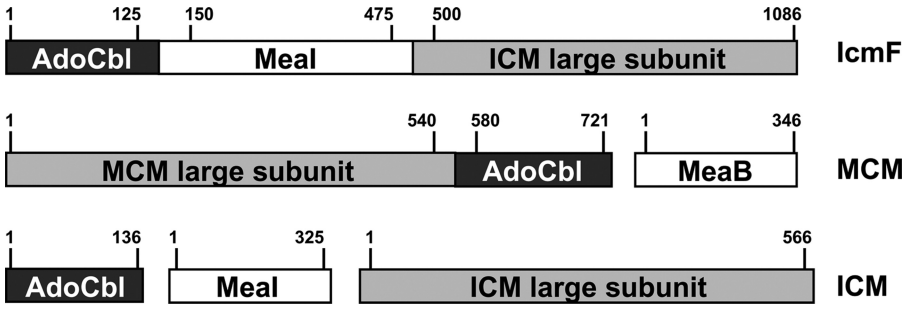

FIGURE 2. **Comparison of domain and gene organizations of bacterial IcmF, MCM, and ICM.** MeaB and MeaI represent the P-loop GTPase chaperones for MCM and ICM, respectively.

icmF from G. kaustophilus—The *icmF* gene from *G. kaustophilus* was amplified from genomic DNA using nested-primer PCR as attempts to amplify the full-length gene in a single PCR were unsuccessful. The first round of PCR was performed with the following primers: forward 5′-TCTACCGATCTGCTAAAGTTCAACG-3′ and reverse 5′-GGATTATGGAGAAACAGCGAGTC-3′. The second round of amplification was performed with the following primers containing NheI and BamHI restriction sites (underlined): forward 5′-TAGGCTAGCATGGCGCACATTTACCGTCCG-3′ and reverse 5′-TAGGGATCCTTACATATTCCGCCGGTATTGTCC-3′.

The resulting fragment was cloned into pGEM-T easy (Promega, WI) and subsequently used as a template for LIC. The insert was amplified with the following primers for LIC cloning, forward 5′-GACGACGACAAGATGGCGCACATTTACCGTCCGAAG-3′ and reverse 5′-GAGGAGAAGCCCGGTTTACATATTCCGCCGGTATTG-3′), and inserted in the pET30 Ek/LIC vector according to the manufacturer's protocol.

icmF from B. xenovorans—The first round of nested-primer PCR was performed on genomic DNA of *B. xenovorans* with the following primers: forward 5′-TGTCGACTTCCTCGCTGAGCGGTT-3′ and reverse 5′-CGCGACGCGTTGTGGTTGTGCGTT-3′. The second round of nested PCRs was performed with primers for LIC: forward 5′-GACGACGACAAGATGACCGATCTGTCCACGCCG-3′ and reverse 5′-GAGGAGAAGCCCGGTTTACATATTGCGGCGGTACTG-3′.

icmF from N. farcinica—The *icmF* gene was amplified from the pTS1 plasmid (genomic DNA clone KNL023_G20) with the following primers containing NdeI and HindIII restriction sites underlined: forward 5′-ATATATCATATGGCCGACAGTACGCTCCACCAA-3′ and reverse 5′-ATATCTAAGCTTTCACACGTTGCGCCGGTACTG-3′. The resulting PCR product was subcloned into the pGEM-T vector (Promega, WI) and used for LIC cloning with the following primers: forward 5′-GACGACGACAAGATGGCCGACAGTACGCTCCAC-3′ and reverse 5′-GAGGAGAAGCCCGGTTCACACGTTGCGCCGGTA-3′. The sequences of all the resulting constructs were verified by nucleotide sequence determination at the Genomics Facility, University of Nebraska.

Protein Expression and Purification

Recombinant *M. elsdenii* butyryl-CoA dehydrogenase expressed in *Escherichia coli* BL21 (DE3) was purified as described previously (20). The pET-30 Ek/LIC vector with the *G. kaustophilus icmF* gene was transformed into *E. coli* BL21 (DE3) cells, which were grown at 37 °C in Luria Bertani (LB) medium containing 50 μg/ml kanamycin to an A_{600} of 0.6. Cells were grown for 14–16 h after induction with 0.5 mM isopropyl 1-thio-β-D-galactopyranoside at 15 °C. The cells were resuspended in ~150 ml of lysis buffer (50 mM sodium phosphate buffer (NaP_i), pH 8.0, 500 mM NaCl, 5 mM dithiothreitol, and 8 mM imidazole) containing three protease inhibitor mixture tablets (Roche Ap-

plied Science) and disrupted by sonication on ice (output setting of 5.5 for 10 min with 30-s bursts and 3-min breaks). Following centrifugation, the cell lysate was subjected to dilution to a final concentration of 3–5 mg/ml and loaded onto a 50-ml nickel-nitrilotriacetic acid-Sepharose column. After washing with 10–20 column volumes of lysis buffer, the protein was eluted with a gradient of 8–250 mM imidazole in lysis buffer. Fractions containing IcmF were pooled, concentrated, and dialyzed against 50 mM NaP_i, pH 7.5, and applied to a 2.5 × 7.5-cm Source 15Q column equilibrated at a flow rate of 10 ml/min with Buffer A (50 mM NaP_i, pH 7.5, 50 mM NaCl). The column was then washed at the same flow rate with 100 ml of Buffer A and eluted with a 500-ml gradient from 50 to 250 mM NaCl in 50 mM NaP_i, pH 7.5, over 50 min at the same flow rate. The purified IcmF was concentrated and loaded on a 160-ml Superdex-200 column (GE Healthcare) equilibrated at a flow rate of 0.75 ml/min with 50 mM NaP_i, pH 7.5, 250 mM NaCl. Under these conditions, IcmF eluted with a retention volume of ~77.5 ml. Fractions containing active IcmF were pooled, concentrated, flash-frozen in liquid nitrogen, and stored at −80 °C until further use. Approximately 25–35 mg of recombinant *G. kaustophilus* IcmF was obtained from a 6-liter culture.

E. coli BL21 (DE3) cells transformed with recombinant *N. farcinica* or *B. fungorum* IcmF were grown, and the cell extracts were prepared as described above for the *G. kaustophilus* enzyme using potassium phosphate (KP_i) buffer. The cell extracts were loaded onto a 4-ml nickel-nitrilotriacetic acid column, washed with 50 mM KP_i, pH 8, containing 50 mM imidazole, and eluted with the same buffer containing 250 mM imidazole. IcmF-containing fractions were pooled, and the protein was obtained in ~40% purity from this one-step purification procedure.

GTPase Activity of IcmF

The GTPase activity of IcmF (5 μM) was determined in the presence of varying concentrations of GTP (50–5000 μM) at 37 °C in 0.4 ml of 50 mM KP_i buffer, pH 7.5, 100 mM KCl, and 5 mM $MgCl_2$. For each GTP concentration, aliquots (50 μl) were removed at varying time points (2–60 min), quenched with 2 M trichloroacetic acid (10% v/v), centrifuged, and filtered through a 0.1-μm Ultrafree-MC filter (Millipore) to remove the precipitated protein.

The nucleotides were analyzed by ion exchange chromatography on a μBondapak NH_2 300 × 3.9-mm high pressure liquid chromatography column (Waters). Initial conditions were 100% Buffer B (50 mM monobasic KP_i, pH 4.5) and 0% Buffer C (800 mM monobasic KP_i, pH 4.5) and a flow rate of 1.0 ml/min. Between 5 and 20 min, Buffer C was increased to 80% and held at that concentration for 5 min. Between 25 and 26 min, Buffer C was decreased to 0% and held for 10 min at that composition to equilibrate the column between injections. Under these conditions, the retention time for GDP was 9.5 min and for GTP was 13.1 min.

Enzyme Assays

Initially, recombinant IcmF was assayed for MCM activity as described previously using the radioactive assay (21). To monitor IcmF activity, one of two assay methods was used. First, a fixed-time GC/MS-based assay was employed by a modification of a method described previously (1, 22). In this assay, normal and isobutyryl-CoA thioesters were saponified, and the resulting free acids were extracted into ethyl acetate. Product formation was followed in a 200-μl assay mixture containing 50 mM KP_i, pH 7.5, 100 mM KCl, normal butyryl-CoA or isobutyryl-CoA (0.1 to 1 mM), 50 μM AdoCbl, and 0.5–5 μg of IcmF. The reaction was stopped by the addition of 100 μl of 2 N KOH containing 0.18 mM valeric acid as an internal standard followed by addition of 100 μl of H_2SO_4 (15%, v/v). In the last step of sample preparation, the reaction mixture was saturated with NaCl and extracted with ethyl acetate (250 μl). An aliquot of the extract (5 μl) was subjected to analysis by GC/MS using a DB-FFAP 30-m × 0.25-mm inner diameter, 0.25-μm capillary column (Agilent, CA). This column is especially designed for the separation of organic acids without derivatization.

A continuous assay was developed to determine the kinetic parameters for IcmF. In this assay, *n*-butyryl-CoA, which is produced from isobutyryl-CoA by IcmF, is converted to crotonyl-CoA by butyryl-CoA dehydrogenase (BDH). BDH activity was followed by the decrease in absorbance at 300 nm over 1–2 min upon reduction of ferricenium hexafluorophosphate ($Fc^+PF_6^-$) ($\Delta\epsilon = 4.3\ mM^{-1}\ cm^{-1}$) (23). BDH is able to use both isobutyryl-CoA and *n*-butyryl-CoA as substrates but with a preference for the latter. We found that with isobutyryl-CoA, $K_m = 311 \pm 26$ μM and $V_{max} = 1.66 \pm 0.06$ units (μmol/min)/mg, and with *n*-butyryl-CoA, $K_m = 68 \pm 4$ μM and $V_{max} = 33 \pm 1$ units/mg. The reaction mixture for the coupled assay contained the following in a final volume of 200 μl: 2–4 μg of IcmF, 50 μM AdoCbl, 0.2 μg of BDH, varying concentrations of isobutyryl-CoA (10–1000 μM), 250 μM ($Fc^+PF_6^-$) ± 1–2 mM GDP, GTP, or GMPPNP in 50 mM NaP_i, pH 7.5, 250 mM NaCl. Under these conditions, the consumption of isobutyryl-CoA by BDH is negligible and similar to the background rate observed in the absence of BDH. The dye was preincubated for 3 min at 37 °C before adding the substrate. After 1 min of incubation, BDH was added, and the reaction was started 1 min later by the addition of holo-IcmF.

UV-visible Spectroscopy

UV-visible spectra were recorded on a Cary 100 spectrophotometer (Varian, Inc., Walnut Creek, CA). Holo-IcmF (10–12 μM) in 50 mM NaP_i, pH 7.5, 0.25 M NaCl ± 5 mM $MgCl_2$, and 1–2 mM GDP, GTP, or GMPPNP was incubated in the presence of 3–5 mM isobutyryl-CoA at 20 °C. The spectra were acquired after 2–5 min of incubation.

Isothermal Titration Calorimetry

The isothermal titration calorimetric experiments were performed as described previously (14, 15). Each experiment was performed in triplicate. IcmF was dialyzed for 10–12 h against 50 mM NaP_i, pH 7.5, 0.25 M NaCl containing 1–2 mM TCEP (Buffer D) before use. The protein (8–24 μM) ± 1–2 mM GDP or GMPPNP in Buffer D was titrated with 30–42 7–9.7-μl aliquots of a 15–20 M excess solution of AdoCbl at 20 °C. The calorimetric signals were integrated, and the data were analyzed with Microcal ORIGIN software using a two-sites binding

model to determine the thermodynamic parameters associated with AdoCbl binding to IcmF.

EPR Spectroscopy

EPR spectra were recorded on a Bruker EMX spectrometer (Bruker Biospin Corp., Billerica, MA), equipped with an Oxford ITC4 temperature controller, a Hewlett-Packard model 5340 automatic frequency counter, and a Bruker gaussmeter. Unless otherwise noted, the following parameters were used: temperature, 100 K; microwave power, 25 milliwatts; microwave frequency, 9.38 GHz; receiver gain, 2×10^5; modulation amplitude, 10 G; modulation frequency, 100 kHz. Cob(II)alamin was generated by treating a solution of hydroxocobalamin with 4–7 molar excess of TCEP. Formation of cob(II)alamin was followed by UV-visible spectroscopy, and the concentration of the solution was estimated using $\epsilon_{473\ nm} = 9.2\ mM^{-1}\ cm^{-1}$.

Bioinformatics Analysis

STRING was used to find functional linkages for proteins of interest, as well as gene fusions and gene neighborhoods (24). A protein-protein blast search (ncbi.nlm.nih.gov) was used to perform distant searching of homologs. A multiple sequence alignment and phylogenetic tree were constructed using a stand-alone version of ClustalX version 1.8. Figures with multiple sequence alignments were generated using BOXSHADE 3.21. Phylogenetic analysis was carried out using default parameters in ClustalX. The trees were visualized using TreeView 1.6.6. Operon and regulon browsers on the Microbes on-line web site were used for the elucidation of functional predictions for the genes of interest (25).

RESULTS AND DISCUSSION

Bioinformatics Analysis of IcmF

Analysis of Mutase Domains—Based on bioinformatics analysis, it was previously concluded that MCM either colocalizes in the same operon with its chaperone, MeaB, or that MeaB is fused to the large subunit of MCM in some bacteria (16). Indeed, the putative fusion protein between MCM and MeaB in *B. xenovorans* was reported to possess MCM activity (16). Our laboratory has been elucidating the influence of MeaB and MCM on the substrate binding and catalytic activities of each other (14). Because the kinetics of a fusion protein are easier to characterize than the stand-alone versions of the component proteins, which interact with varying affinities depending on the ligand, we chose to focus on the putative MCM-MeaB fusion protein. A BLAST search using the fusion protein from *B. xenovorans* (NCBI code YP_556774) as a query sequence resulted in the identification of >70 proteins in bacteria, including the seven proteins that were previously identified as examples of fusions between MCM and MeaB (supplemental Table S1) (16). In the data bases, homologs of this fused protein are annotated as putative MCM-like proteins. However, a careful examination of the domain organization and sequence analysis of the substrate-binding site in the B_{12}-dependent isomerase component (Figs. 2–4) suggested that this group of fusion proteins might in fact be misannotated.

Based on the high sequence similarity between MCM and ICM, Robinson and co-workers (2) used the crystal structure of MCM from *Propionibacterium shermanii* to identify residues that might be involved in specific substrate binding in ICM from *S. cinnamonensis*. They identified two key substitutions in the large subunit of MCM, Tyr-89 and Arg-207, which are replaced by Phe-80 and Gln-198 in the large subunit of ICM (Fig. 3). These differences in active site residues can be rationalized based on the structural difference between the respective substrates despite the very similar reactions catalyzed by the two enzymes (Fig. 1). In MCM, the carboxylate group of methylmalonyl-CoA is engaged in electrostatic interactions with the guanidinium group of Arg-207 and the phenolic group of Tyr-89 (Fig. 3). The presence of a methyl group in the ICM substrates instead of the carboxylate is reflected in the loss of the hydrogen bond donating arginine and tyrosine residues. Instead, a glutamine and phenylalanine in ICM substitute for the arginine and tyrosine residues, respectively in MCM (Fig. 3). Apart from these two differences, the remaining residues in the active sites of both mutases are highly conserved.

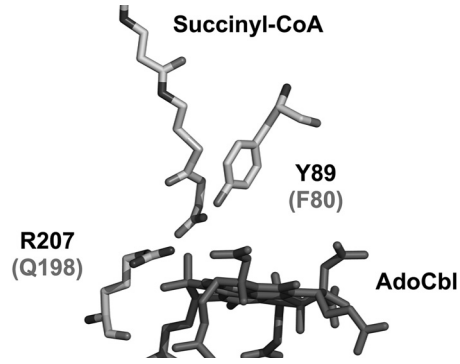

FIGURE 3. **Comparison of the active site residues in *P. shermanii* MCM with those predicted for *S. cinnamonensis* ICM.** The MCM structure was obtained from the Protein Data Bank code 4REQ. The two striking differences in the active site residues are the substitutions of Tyr-89 and Arg-207 in MCM by Phe-80 and Gln-198 in ICM.

Multiple sequence alignment of the predicted substrate-binding site in the C termini of all the identified fusion proteins clearly reveals conservation of the Phe and Gln residues (Fig. 4 and supplemental Fig. S1). This analysis strongly suggests that the substrate for the fusion protein is *n*-butyryl-CoA/isobutyryl-CoA, and hence the fusion protein is predicted to be an ICM and not an MCM. We thus designate this fusion protein as IcmF, for isobutyryl-CoA mutase fused. The IcmF designation for this group of fusion proteins also distinguishes it from the "stand-alone" ICM described for the genus *Streptomyces*.

All IcmFs are predicted to be composed of three domains as follows: the N-terminal AdoCbl binding region that is homologous to the small subunit of ICM, a middle P-loop GTPase domain, and a C-terminal region that is homologous to the large substrate-binding subunit of ICM (Fig. 2). Clear sequence similarities are seen between the AdoCbl binding regions of the large subunit of MCM, the small subunit of ICM (IcmB), and the N-terminal portion of IcmF (Fig. 5). The signature D*X*H*XX*G…S*X*L…GG motif (where *X* is any amino acid) used for binding B_{12} in the "base-off/His-on" conformation is observed in all three proteins (5). However, in IcmF, this motif is similar but not identical to that seen in ICM and MCM. First, a Gly → Ala/Ser change is found in IcmFs in the following

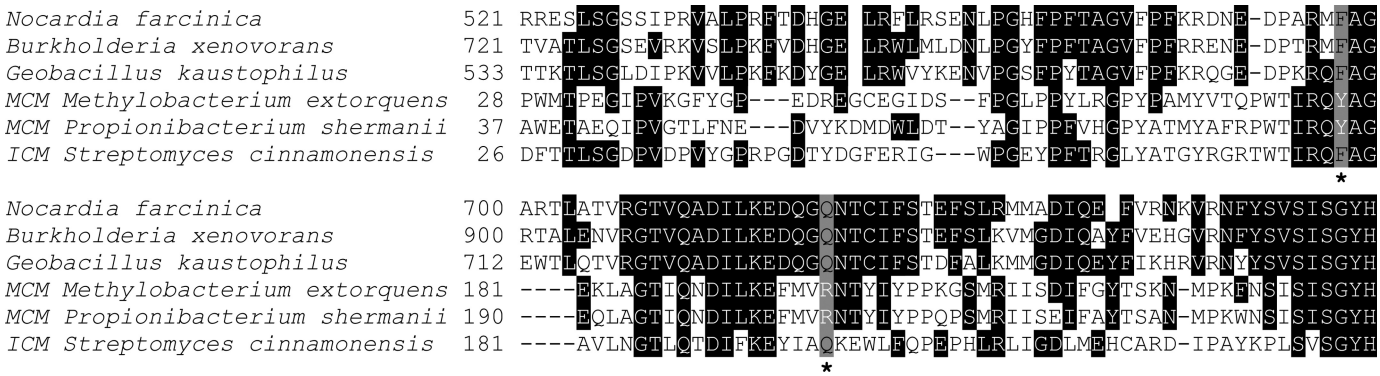

FIGURE 4. **Multiple sequence alignment of the C-terminal sequences of IcmFs, the large subunit of ICM (IcmA) from *S. cinnamonensis* (AAC08713), MCM from *M. extorquens* (YP_001642233), and MCM from *P. shermanii* (CAA33090).** The C-terminal region of the IcmFs is homologous to IcmA and MCM. The two conserved residues in IcmF (Phe and Gln-1 in IcmA) that are important for substrate binding are highlighted in *gray* and indicated with *asterisks*. In MCM, these residues are substituted by Tyr and Arg, respectively. The sequence alignment for a more extensive list of putative IcmFs is shown in supplemental Fig. S1.

conserved sequence: D*X*H*XX*(A/S)…S*X*Y..GGGG. This substitution is not surprising because glycine is often replaced by alanine or serine and vice versa in sequences of orthologous proteins from different organisms. Second, an S*X*L→S*X*Y substitution is seen in IcmF. The rationale for the leucine to tyrosine substitution and the insertion of two glycines at the end of the motif are not clear. Thus, it appears that the sequence of the AdoCbl binding domain of IcmF has diverged from the corresponding sequences in IcmB and MCM.

Analysis of G-protein Domains—The P-loop GTPase domain has very high sequence similarity to MeaB from *M. extorquens* that was shown to be a chaperone for MCM (14, 15). We designated it as MeaI to distinguish it from the MeaB-like chaperone. The sequence encoding the MeaI domain of IcmF includes ~250–300 amino acids in the middle of the protein (Fig. 6). Sequence analysis strongly suggests that this domain belongs to the G3E family of P-loop GTPases (10). All four GTPase sequence fingerprints, the so-called G domains, which define this family, are present in the MeaI domain of IcmF. These include the following: (i) the Walker A motif (G1), which binds the triphosphate moiety of GTP (as is typical for the G3E subfamily, a slight modification of the G*XXGX*GK(ST) sequence to G*XXGX*GK(SS) is seen); (ii) the Mg^{2+}-binding motif (G2) (L*XX*D in all IcmF sequences); (iii) the D*XXXX*E*XX*G Walker B motif (G3); and (iv) the nucleotide specificity NK*X*D motif (G4). The replacement of Asp by Glu in NK*X*D motif in some proteins (Fig. 6) might not affect the specificity for the guanine nucleotide and is also seen in other G-proteins (26). Based on this analysis, we conclude that the MeaI domain of IcmF, like MeaB, belongs to the SIMIBI subclass of G-proteins because two key aspartate residues at the N terminus of the Walker B motif and in the Mg^{2+}-binding motif are present (Fig. 6). Within the SIMIBI subclass, the MeaI domain of IcmF belongs to the G3E family (the conserved glutamate residue in the Walker B motif is a signature of this family) as well as the intact nucleotide specificity motif (10). We predicted that the MeaI domain of IcmF functions like its paralog MeaB, *i.e.* as a chaperone for ICM in the fusion protein (14).

Expression and Initial Activity Analysis of IcmF

To test the prediction from bioinformatics analysis that IcmF harbors ICM rather than MCM activity, the *icmF* gene from three organisms, *G. kaustophilus*, *B. xenovorans,* and *N. farcinica,* were cloned into the expression vector pET30 Ek/LIC. Multiple IcmF-encoding genes were subcloned and purified so that the enzymatic activity of the fusion protein from more than one organism could be assessed.

Because the fusion protein from *B. xenovorans* was reported to have MCM activity (16), we initially tested the activity of all three IcmF proteins in the standard radiolabeled assay for MCM (21). However, none of the three IcmFs exhibited detectable MCM activity. On the other hand, all three IcmFs exhibited ICM activity. Two assays have been described for monitoring ICM activity and are based on either gas chromatography (GC) or NMR-based detection of the reactant and product (27). Because the NMR-based method is not amenable for routine enzymatic assays, we used a modification of the previously described GC assay (1, 22) using mass spectrometry (MS) for detection of the reaction components. A specific activity of 0.6 ± 0.04 μmol min^{-1} mg^{-1} protein at 37 °C was obtained for the *G. kaustophilus* IcmF.

As an alternative to the gas chromatography-mass spectrometry assay that depends on access to specialized instrumentation, a coupled spectrophotometric assay was developed to measure IcmF activity as described under "Experimental Procedures." The specific activity determined in the coupled assay for the *N. farcinica* IcmF was 1.1 ± 0.1 μmol min^{-1} mg^{-1} and for the *B. xenovorans* IcmF was 0.34 ± 0.04 μmol min^{-1} mg^{-1} at 37 °C. A specific activity of 0.75 ± 0.01 μmol min^{-1} mg^{-1} protein at 37 °C was measured for *G. kaustophilus* IcmF, which is comparable with the value from the gas chromatography-mass spectrometry assay. In comparison, a V_{max} of 38 ± 3 μmol min^{-1} mg^{-1} at 37 °C has been reported for purified stand-alone ICM from *S. cinnamonensis* (2).

The recombinant *G. kaustophilus* IcmF was the most stable and soluble of the three proteins and was further purified to ~95% purity as described under "Experimental Procedures" to perform biochemical and biophysical characterizations. Based on its elution from a calibrated gel filtration column, the *G. kaustophilus*

IcmF appears to be a dimer with a native molecular mass of ~286 kDa.

Binding of AdoCbl to IcmF ± Nucleotides

We investigated the energetics of AdoCbl binding to *G. kaustophilus* IcmF ± nucleotides by Fig. 7 and Table 1. These experiments revealed the presence of two nonequivalent binding sites with an ~9–25-fold difference in affinity for AdoCbl that was influenced by the presence and identity of the guanine nucleotide (Table 1). Binding of AdoCbl to the high affinity site in the absence of nucleotides (K_D = 81 ± 14 nM) is accompanied by a ΔG_1^0 of −9.5 ± 0.1 kcal/mol that is enthalpically favored, whereas binding to the low affinity site (K_D = 2.0 ± 0.4 μM) is entropically driven (Table 1). These data suggest a possible difference in the flexibility of the two AdoCbl-binding sites in IcmF. A K_{act} of 12 ± 2 μM for AdoCbl for ICM from *S. cinnamonensis* has been reported (2).

We next analyzed the influence of nucleotides on cofactor binding. The affinity for AdoCbl for the high affinity site was slightly increased in the presence of GDP (132 ± 9 nM), which resulted from changes in both enthalpic and entropic contributions ($\Delta\Delta H_1$ ~2.5 kcal/mol and $\Delta T\Delta S_1$ ~2.8 kcal/mol). GDP did not substantially influence binding of AdoCbl to the second site. Binding of AdoCbl in the presence of GMPPNP, a nonhydrolyzable analog of GTP (Fig. 7 and Table 1), indicates that GTP hydrolysis is not required for binding of AdoCbl to IcmF·GTP. GMPPNP decreased by ~2-fold the affinity for AdoCbl to site 1 (K_{D1} = 154 ± 71 nM) and slightly increased the affinity at site 2 (K_{D2} = 1.3 ± 0.5 μM). Changes in both the enthalpic and entropic terms contributed to this change. Although cofactor binding to site 1 is enthalpically driven, it is almost entirely entropically driven at site 2.

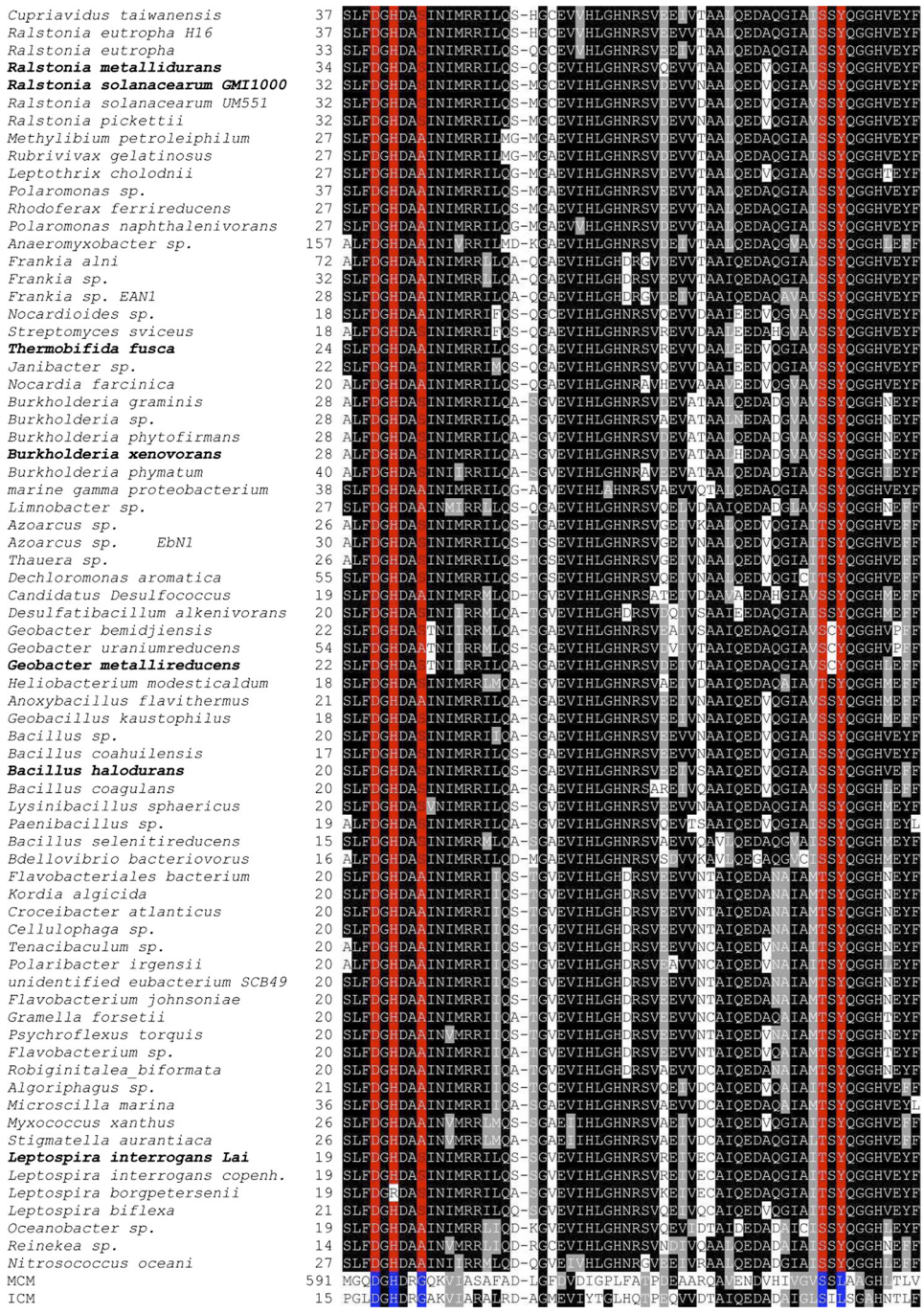

FIGURE 5. **Multiple sequence alignment of the N-terminal AdoCbl binding domain of IcmFs, the small subunit of ICM (IcmB) from *S. cinnamonensis* (CAB59633), and MCM from *M. extorquens* (YP_001642233).** In B_{12} proteins that bind the cofactor in a base-off/His-on conformation, a signature …*SXL*…GG motif is found (highlighted in *blue*). In IcmF, this motif is similar but not identical as follows: D*XHXX*(A/S)…(S/T)*XY*…GGGG (highlighted in *red*). In *Leptospira borgpetersenii*, the histidine that is predicted to coordinate to AdoCbl appears to be substituted by arginine. The *Salinibacter ruber* sequence is not included in the alignment because the AdoCbl region is truncated at the N terminus (D*XHXX*G motif is missing). IcmFs, which were previously annotated as MCM-like enzymes, are indicated in *boldface*. For accession numbers see supplemental Table S1.

IcmF Is an Active Isobutyryl-CoA Mutase

Using the coupled assay, we further characterized the kinetic parameters for IcmF from *G. kaustophilus* (Fig. 8*A* and Table 2). The K_m value for isobutyryl-CoA was determined to be 20 ± 1 μM and the k_{cat} to be 3.1 ± 0.1 s^{-1} in the absence of nucleotides. In comparison, for isobutyryl-CoA a K_m of 57 ± 13 μM has been reported for ICM from *S. cinnamonensis* (2). Thus, the k_{cat}/K_m values for the stand-alone *S. cinnamonensis* ICM and *G. kaustophilus* IcmF are 6.8 ± 2.7 × 10^5 M^{-1} s^{-1} (2) and 1.5 ± 0.1 × 10^5 M^{-1} s^{-1} respectively. We note that the activity of the

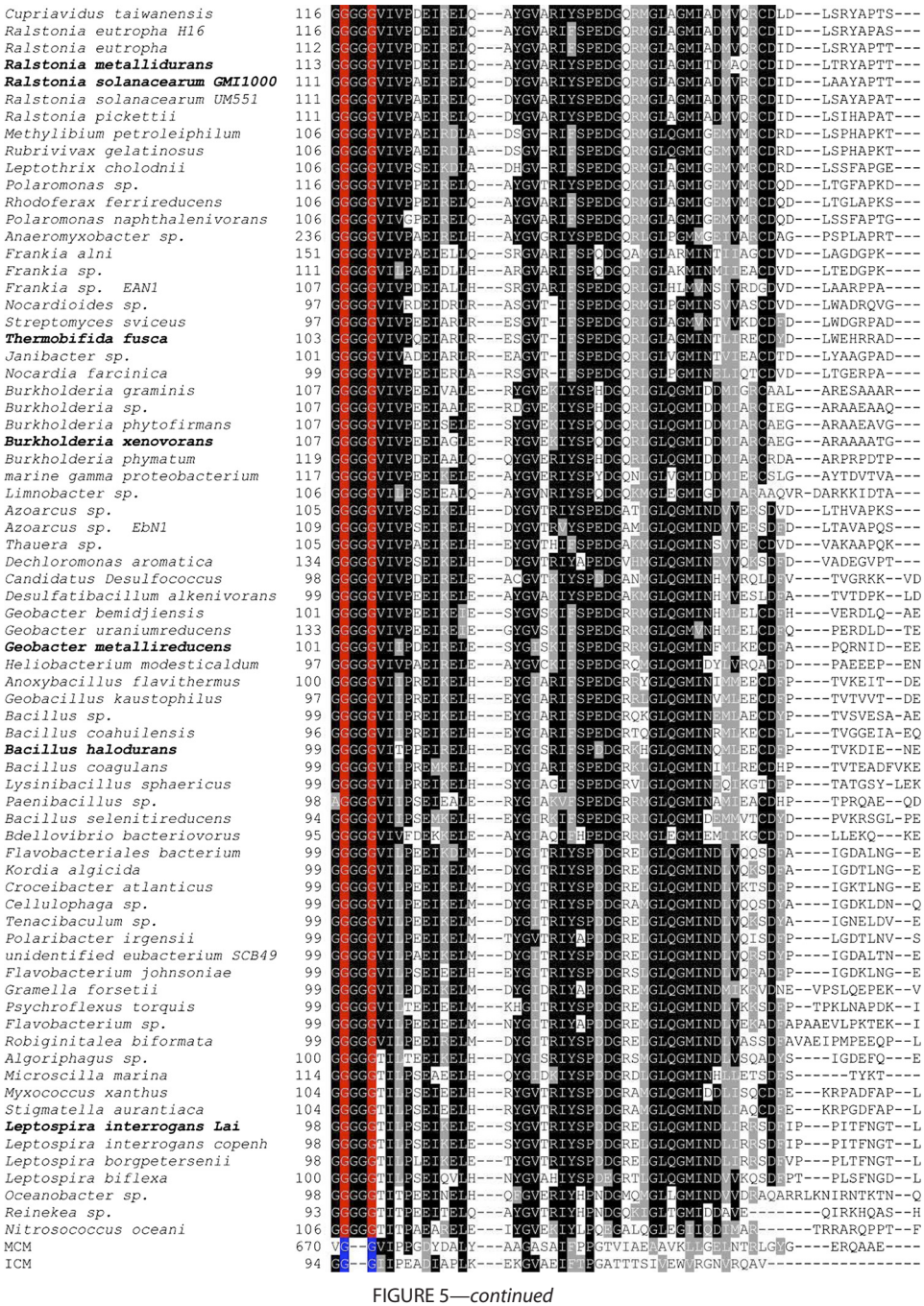

FIGURE 5—*continued*

G. kaustophilus was measured at 37 °C in the coupled enzyme assay, which is significantly lower than the optimal growth temperature (60 °C) for the organism (28). Because purified recombinant IcmF was found to be unstable at higher temperatures, its activity at 60 °C could not be measured. Based on a coefficient of 2 for every 10 °C rise in temperature, we estimate that the k_{cat} for this enzyme might be ~4-fold higher at 60 °C.

Surprisingly, the presence of GDP or GTP affected both the k_{cat} and K_m values (Fig. 8*A* and Table 2). Thus, the presence of nucleotides decreased k_{cat} ~1.6–1.7-fold while increasing the K_m ~2-fold. Consequently, the catalytic efficiency k_{cat}/K_m value of IcmF decreased 3.5- and 4-fold, respectively, in the presence of GDP and GTP.

Absorption Spectroscopy of IcmF under Steady-state Turnover Conditions

As IcmF like ICM is expected to deploy radical chemistry with AdoCbl (Fig. 1), we analyzed whether the presence of nucleotides affected the cob(II)alamin levels under steady-state turnover conditions (Fig. 8*B*). In the presence of isobutyryl-CoA, the spectrum of holo-IcmF was a ~1:2 mixture of cob(II)alamin:AdoCbl. In the presence of nucleotides, accumulation of cob(II)alamin was diminished to ~1:4 (GDP) and ~1:9 (GMPPNP) (Fig. 8*B*). These results indicate that the nucleotides influence the steady-state distribution of intermediates, which might be related to their effects on k_{cat}.

EPR Spectroscopy

The existence of a biradical intermediate has been demonstrated by EPR spectroscopy for MCM from *P. shermanii* with cob(II)alamin coupled to the product radical (29). However, an EPR spectrum was not observed when 40 μM holo-IcmF was mixed with 7 mM isobutyryl-CoA and frozen rapidly. Because the cob(II)alamin intermediate is observed by UV-visible spectroscopy (Fig. 8*B*), the lack of a paramagnetic signal suggests strong coupling between it and the organic radical species in the IcmF active site. This has also been observed with MCM from *M. extorquens*.[4]

The EPR spectrum of cob(II)alamin bound to IcmF was recorded (Fig. 8*C*). Binding of cob(II)alamin by IcmF yields an EPR spectrum that is diagnostic for the presence of an axial nitrogen ligand. Hyperfine coupling between the unpaired electron and the $S = 7/8$ cobalt nucleus results in an eight-line spectrum, which is further split into triplets due to superhyperfine coupling to the $I = 1$ axial nitrogen ligand (Fig. 8*C*, *spectrum 1*). The spectrum of cob(II)alamin bound to IcmF differs from that of free cob(II)alamin (Fig. 8*C*, *spectrum 4*) particularly in the *S*-shaped absorption feature at $g \approx 2.3$ and probably results from immobilization of the cofactor in the active site. When IcmF was reconstituted with cob(II)alamin and 5′-deoxyadenosine in the presence or absence of isobutyryl-CoA (Fig. 8*C*, *spectra 2* and *3*), the spectra showed sharpening and resolution of additional hyperfine struc-

[4] D. Padovani and R. Banerjee, unpublished results.

ture in the *S*-shaped feature was observed. These spectral differences suggest conformational changes that influence the electronic properties of the cob(II)alamin radical.

GTPase Activity of IcmF

Because IcmF possesses an MeaI-like domain, it was expected that this protein, like MeaB, can hydrolyze GTP. Hence, the kinetics of GTP hydrolysis catalyzed by apo-IcmF was characterized. A Michaelis-Menten analysis of the data yielded the following parameters: $K_{m(GTP)} = 51 \pm 3\ \mu M$ and $k_{cat} = 1.8 \pm 0.05\ min^{-1}$ (Fig. 8*D*). In comparison, MeaB alone exhibits a lower intrinsic GTPase activity ($k_{cat} = 0.039 \pm 0.003\ min^{-1}$), which is increased ~100-fold in the presence of MCM (15).

MeaI Domain of IcmF Is Distinct from MeaB

The phylogenetic relationship between MeaB, the chaperone for MCM, and the MeaI domain of IcmF was evaluated. A dendrogram constructed from the analysis of MeaB and MeaI sequences found in the same organisms reveal that the two gene groups cluster separately (Fig. 9). MeaB and MeaI are thus paralogs that have evolved to serve specific partner proteins, *i.e.* MCM and ICM.

The observation of a MeaI domain in IcmF raises the obvious question of whether MeaI chaperones also exists for stand-alone ICMs. Indeed, as discussed below, analysis of genomic sequence reveals that two MeaB-like proteins are found in bacterial genomes, one associated with MCM (MeaB) and the other with ICM (MeaI). The diversification of the G domain sequences within each subgroup strongly suggests that the MeaI-like domain of IcmF is evolutionarily distinct from MeaB related to MCM.

Identification of Stand-alone ICMs That Do Not Belong to the Genus Streptomyces

To investigate the relationships between the chaperones for ICM *versus* IcmF, we analyzed other bacterial genomes for the presence of stand-alone ICMs and MeaIs. In our search we assumed the following: (i) the *icmA* and *icmB* genes are not necessarily located close to each other, and (ii) the amino acid substitutions corresponding to Phe-80 and Gln-198 in the *S. cinnamonensis* sequence are always found

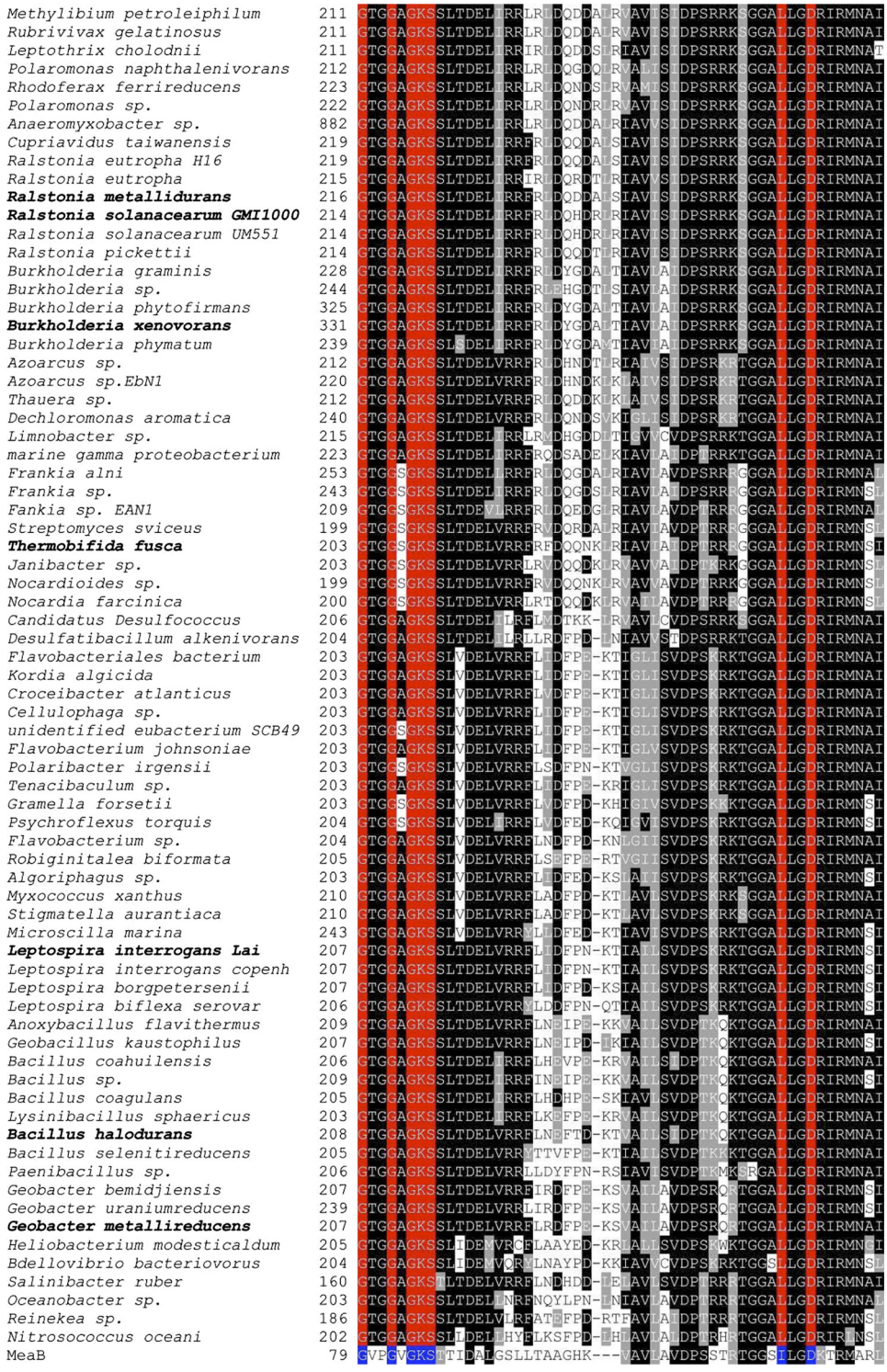

FIGURE 6. **Multiple sequence alignment of the MeaI domain in IcmF sequences and MeaB from *M. extorquens* (YP_001637793).** The MeaI domain of IcmF includes ~250–300 amino acids in the middle of the protein. Sequence analysis strongly suggests that this domain belongs to the G3E family of P-loop GTPases. The G domains, which define this family, are present in the MeaI domain of IcmF and are highlighted in *red*. These include the following: (i) the Walker A G*XX*G*X*GK(SS) motif; (ii) the Mg^{2+}-binding motif, which is typically (V/I)*XX*D in proteins in the G3E family and is L*XX*D in all IcmF sequences; (iii) the D*XXXX*E*X*G Walker B motif; and (iv) the nucleotide specificity NK*X*(D/E) motif. IcmFs, which were previously annotated as MCM-like enzymes, are indicated in *boldface*. For accession numbers see supplemental Table S1.

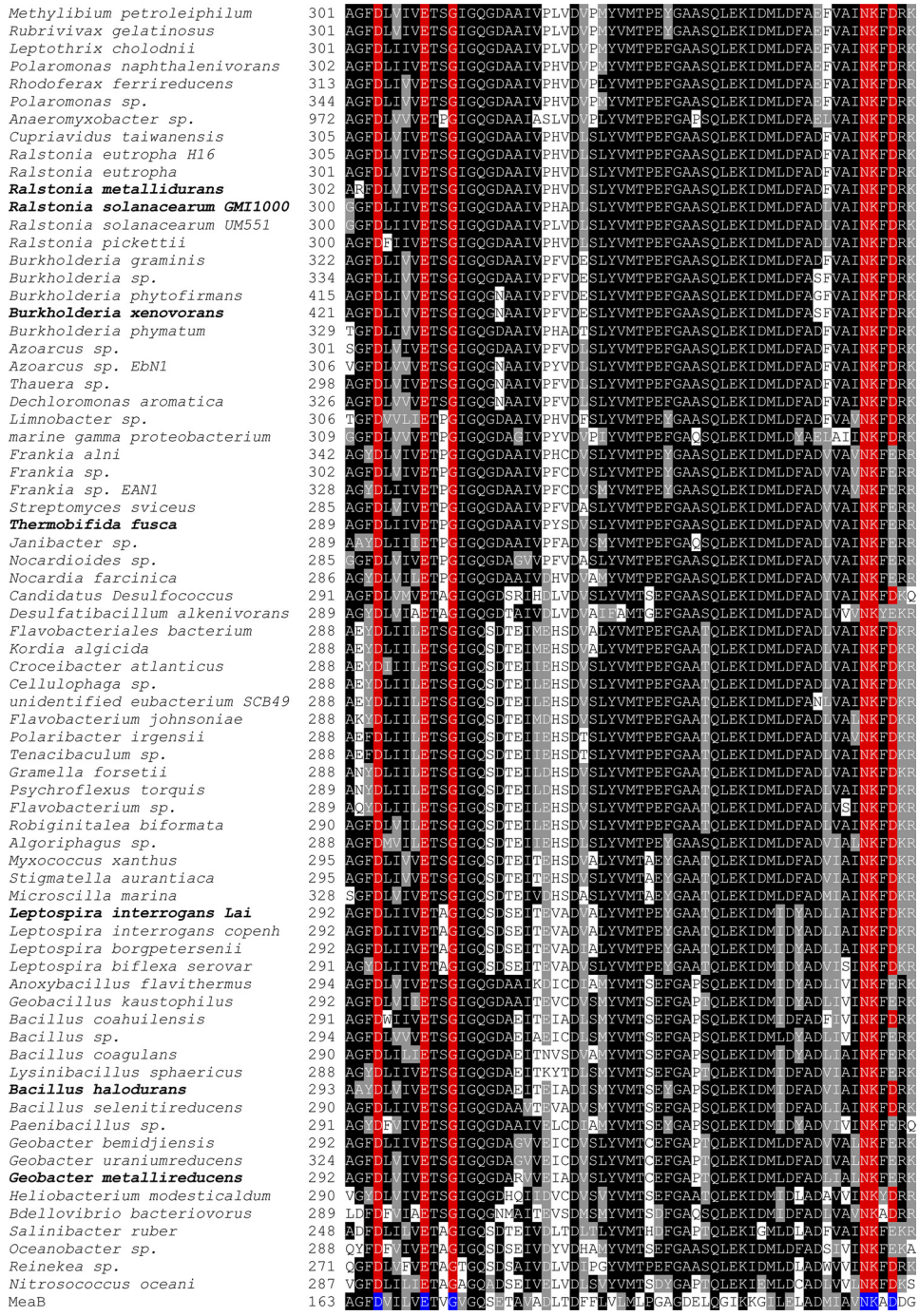

FIGURE 6—*continued*

in the large subunit of ICM. A BLAST search using both subunits of the stand-alone ICM from *S. cinnamonensis* as the query sequence identified several stand-alone ICM sequences, primarily in thermophilic archaea but also in halophilic archaea and in a limited number of bacteria (supplemental Table S2 and supplemental Fig. S2). Furthermore, using the MeaI domain of IcmF as a query sequence revealed that genes encoding stand-alone MeaIs can be associated with either the large or the small subunit of ICM (supplemental Table S2). Interestingly, in several organisms, both ICM subunits are localized in the same operon or are in close proximity, *e.g.* in *Desulfitobacterium hafniense*, *Archaeoglobus fulgidus*, and *Symbiobacterium thermophilum*. However, in other organisms, the two subunits are not close to each other in the genome, *e.g.* in *Haloarcula marismortui*, *Halobacterium* sp., and in *Natronomonas pharaonis* (supplemental Table S2). In some organisms, the gene order in an ICM-encoding operon is the following: MeaI, small subunit of ICM, large subunit of ICM, and in others the small subunit and MeaI colocalize in an operon whereas the large subunit is independently transcribed.

A phylogenetic tree based on the alignment of stand-alone MeaIs, the MeaI domain of IcmF and the MeaBs associated with MCM, reveals significant overall similarity between these proteins (supplemental Fig. S3). However, a careful examination of all available MeaI sequences reveals that this group is evolutionarily distinct from MeaB because they form two separate clusters in the dendrogram. In contrast, MeaIs associated with stand-alone ICMs are closely related to the corresponding domain in IcmF. Hence, the MeaI and MeaB are paralogs that probably evolved from a common ancestor and have diverged to support specific B_{12}-dependent isomerases.

Implications of the Presence of IcmF

Gene fusion events occur during evolution resulting in the physical coupling of functionally coupled proteins. It is speculated that gene fusions that facilitate functional interactions between and/or coregulation of proteins might be maintained by selective pressure and are more common than gene fissions (30, 31). In this study, we have characterized IcmF, a protein that likely arose by fusion of three genes encoding the large and small subunits of ICM and the chaperone MeaI. Bioinformatics analysis has allowed identification of >70 IcmFs in bacterial and archaeal genomes. However, as noted earlier, all these proteins are incorrectly assigned as representing fusions between MCM and MeaB. There are several reasons that could have led to misannotation of IcmF in the data bases. First, ICM activity was believed to be restricted to the genus *Streptomyces*, whereas the MCM-catalyzed reaction is important in secondary metabolism and is widely distributed in bacteria. Second, the two signature active site substitutions in the *S.*

cinnamonensis ICM was missed in the IcmF sequence (16). The importance of these residues in substrate selectivity was previously demonstrated by mutagenesis studies in which the MCM double mutant, Y89F/R207Q, was designed to mimic the active site residues in ICM (32). In contrast to wild-type MCM, the double mutant bound the ICM substrates, *n*-butyryl-CoA or isobutyryl-CoA, but instead of catalyzing an isomerization it led to inactivation via an internal electron transfer.

Third, the role for a MeaB-like chaperone protein has only been described so far for MCM and could have contributed to the erroneous assignment. IcmF (previously described as McmC) was reported to have very low MCM activity ($10–12 \times 10^{-3}$ μmol min^{-1} mg^{-1}) in crude extracts of *B. xenovorans*, an organism that lacks the gene encoding a stand-alone MCM (16). However, when we cloned and purified the *B. xenovorans* IcmF, we found it to be devoid of MCM activity, which in fact, prompted a closer inspection of the protein sequence and therefore its predicted activity.

Our findings expand our view of the distribution of B_{12}-dependent mutases. We find that ICM activity is much more widely distributed in nature than previously suspected and raises questions about the metabolic pathways in which this activity is involved.

In certain bacteria (*e.g. Butyrivibrio fibrisolvens* and *Streptomyces collinus*), acetyl-CoA is converted to butyryl-CoA via four reactions, involving acetyl-CoA acetyltransferase (thiolase), 3-hydroxybutyryl-CoA dehydrogenase, 3-hydroxybutyryl-CoA dehydratase (crotonase), and butyryl-CoA dehydrogenase (33–35).

Subjecting the IcmF sequences to operon analysis reveals that in eight bacterial genomes (*Lysinibacillus sphaericus*, *Bacillus* sp., *Bacillus halodurans*, *Bacillus coagulans*, *Bacillus selenitireducens*, *Bdellovibrio bacteriovorus*, *Geobacillus* sp., and *Anoxybacillus flavithermus*) IcmF is located in the same operon with enzymes involved in formation of butyryl-CoA from acetyl-CoA. Based on this analysis, we posit that IcmF is involved in butyryl-CoA, rather than methylmalonyl-CoA metabolism in these bacteria.

Myxalamids are inhibitors of the eukaryotic electron transfer chain that are produced by the myxobacteria, *Myxococcus xanthus* and *Stigmatella aurantiaca* (36). In studies on *M. xanthus* and *S. aurantiaca* mutants in which the branched-chain ketoacid dehydrogenase was disrupted (*bkd* mutants), it was shown that isobutyryl-CoA is incorporated into the final product (37). These results were unexpected because the *bkd* mutants are unable to form isobutyryl-CoA starter units from valine. The authors suggested that fatty acid degradation by α- and β-oxidation of iso-odd fatty acid could be responsible for isobutyryl-CoA synthesis (37). We speculate that the ICM activity of IcmF found in both these bacteria might play a role in this process instead.

Another interesting implication of our study stems from the identification of stand-alone ICMs in a number of archaea and bacteria (supplemental Table S2 and supplemental Fig. S2). Recently, Fuchs and co-workers (17, 38) have reported the discovery of a novel CO_2-fixation pathway in several archaea. They have characterized the 16 enzymes in the 3-hydroxypropionate/4-hydroxybutyrate pathway in *Metallosphaera sedula*. In this pathway, two CO_2 molecules are fixed with acetyl-CoA and reductively converted to succinyl-CoA. An intermediate step in this pathway is the conversion of methylma-

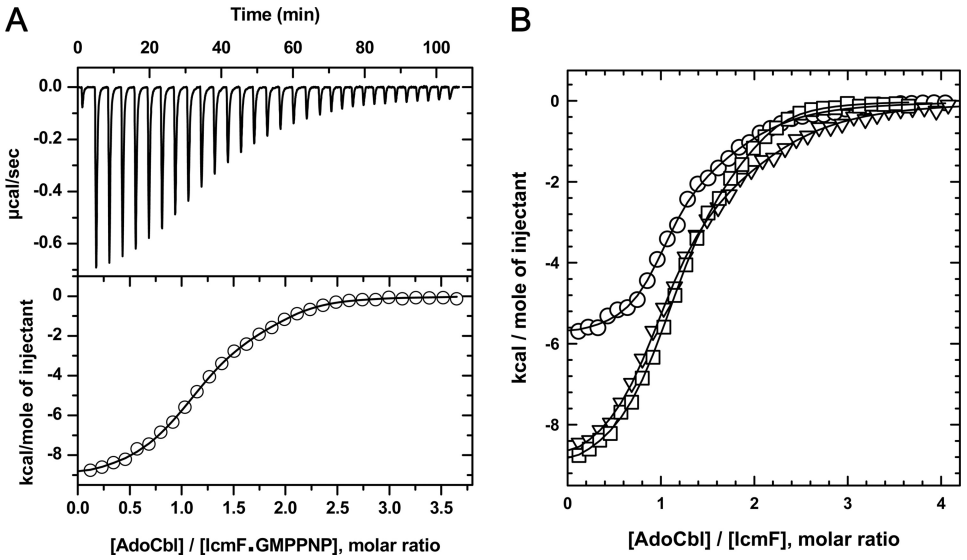

FIGURE 7. **Binding isotherms for AdoCbl binding to IcmF.** *A,* representative isothermal titration calorimetry data set for the binding of AdoCbl (250 μM stock solution) to 15.4 μM apo-IcmF in 50 mM sodium phosphate buffer, pH 7.5, 250 mM NaCl, 2 mM TCEP at 20 °C. *B,* titration curves for the binding of AdoCbl to apo-IcmF alone (○) and in the presence of 1 mM GDP (▽) or 1 mM GMPPNP (□). Data were fitted to a two-site model and yielded the parameters reported in Table 1.

TABLE 1

Thermodynamic parameters for the binding of AdoCbl to IcmF

All experiments were performed in 50 mM NaP_i, pH 7.5, 250 mM NaCl, 1–2 mM TCEP at 20 °C as described under "Experimental Procedures." The data represent the mean ± S.D. of three independent experiments.

Ligand	Site	*n*	K_d	ΔH	$T+\Delta S$	ΔG
			μM	kcal/mol	kcal/mol	kcal/mol
None	1	0.9 ± 0.1	0.081 ± 0.014	−6.2 ± 0.2	+3.4 ± 0.3	−9.5 ± 0.1
	2	1.0 ± 0.2	1.98 ± 0.42	−2.0 ± 0.9	+5.6 ± 1.0	−7.7 ± 0.1
GDP	1	0.9 ± 0.1	0.132 ± 0.009	−8.7 ± 0.7	+0.6 ± 0.8	−9.2 ± 0.1
	2	1.2 ± 0.1	2.77 ± 1.27	−2.4 ± 0.3	+5.1 ± 0.4	−7.5 ± 0.2
GMPPNP	1	1.0 ± 0.1	0.154 ± 0.071	−9.6 ± 0.1	−0.4 ± 0.4	−9.2 ± 0.3
	2	1.0 ± 0.1	1.30 ± 0.51	−0.5 ± 0.7	+7.4 ± 0.5	−7.9 ± 0.2

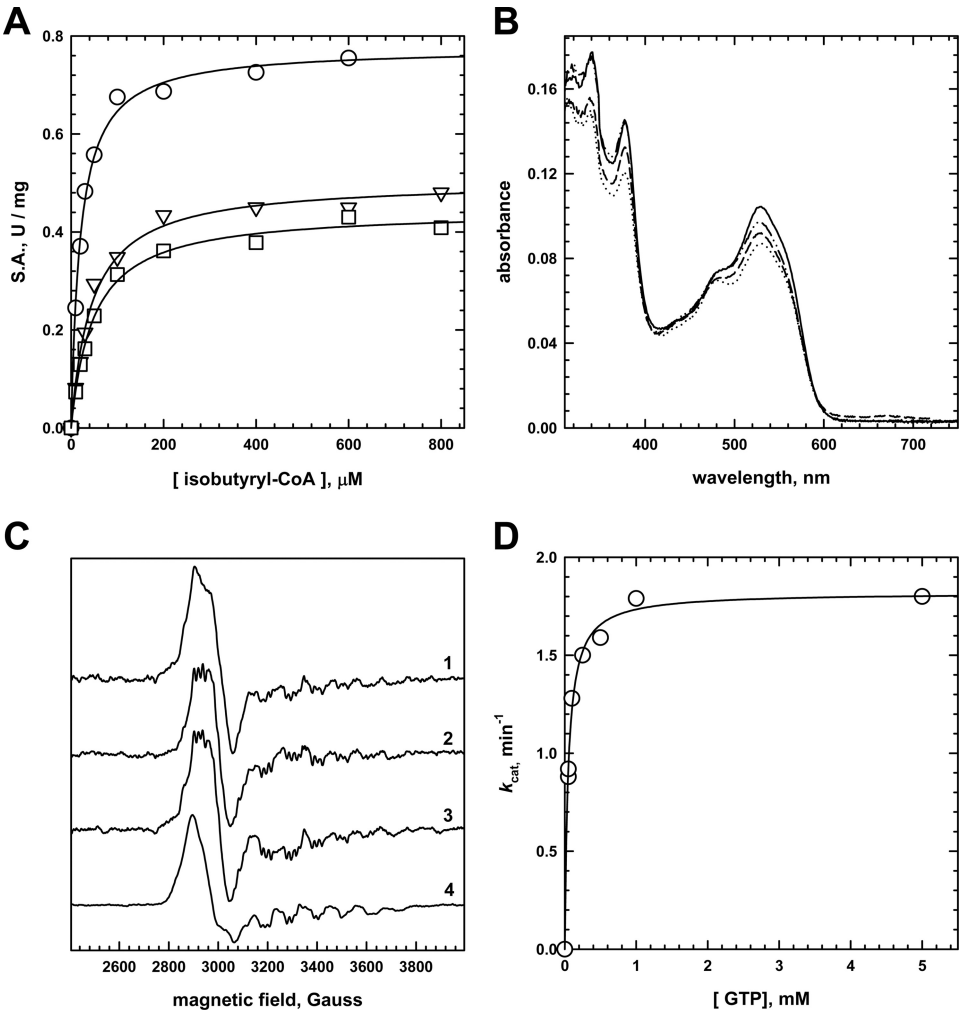

FIGURE 8. **Kinetic and spectroscopic characterization of IcmF.** *A,* Michaelis-Menten analysis of the IcmF reaction as determined in the coupled enzyme assay. The specific activity (*S.A.*) of IcmF, analyzed alone (○) or in the presence of GDP (▽) or GTP (□), yielded the kinetic parameters reported in Table 2. *B,* UV-visible spectra of holo-IcmF under steady-state turnover conditions. Holo-IcmF (10.3 μM, *solid line*) was incubated at 20 °C for 2 min with 3.4 mM isobutyryl-CoA (*dotted line*) in the presence of 2 mM GDP (*dashed line*) or GMPPNP (*dashed-dotted line*). *C,* EPR spectra of IcmF (28 μM) reconstituted with 20 μM cob(II)alamin (*spectrum 1*) in the presence of 10 mM 5′-deoxyadenosine (*spectrum 2*) and 8 mM isobutyryl-CoA (*spectrum 3*). An EPR spectrum of free "base-on" cob(II)alamin (*spectrum 4*) is shown for comparison. *D,* Michaelis-Menten analysis of the GTPase activity of IcmF determined as described under "Experimental Procedures."

TABLE 2

Kinetic parameters for IcmF

All experiments were performed in 50 mM NaP_i, pH 7.5, 250 mM NaCl at 37 °C as described under "Experimental Procedures." The data represent the mean ± S.D. of three independent experiments.

Nucleotide	None	GDP	GTP
K_m (isobutyryl-CoA), μM	20.1 ± 1.3	45.3 ± 4.0	50.8 ± 2.6
k_{cat}, s^{-1}	3.10 ± 0.05	1.96 ± 0.04	1.88 ± 0.08
k_{cat}/K_m, M^{-1} s^{-1}	(1.5 ± 0.1) × 10^5	(4.3 ± 0.5) × 10^4	(3.7 ± 0.4) × 10^4

lonyl-CoA to succinyl-CoA, which is catalyzed by MCM. The majority of MCMs in bacteria are heterodimers, in which one of the subunit binds the substrate and the cofactor. Although *M. sedula* clearly encodes MCM in its genome, some of the putative mutases in other organisms that were identified as MCMs (see supplemental Table S1 in Ref. 17) are predicted to be stand-alone ICMs based on the Tyr → Phe/Arg → Gln substitutions in their active sites. Thus, in *H. marismortui*, *Halobacterium* sp., and *N. pharaonis* stand-alone ICMs rather than MCMs are predicted to exist, raising questions about the presence of an intact 3-hydroxypropionate/4-hydroxybutyrate pathway in these organisms (supplemental Fig. S2). In contrast, in *A. fulgidus* and *Halorubrum lacusprofundi* both copies of the *mcm* and *icm* genes are present. In *M. sedula,* only one copy of MCM is present (supplemental Fig. S2). Fuchs and co-workers (17) noted that in some organisms the enzymes from the first half of the cycle are missing and proposed that in this situation reversal of the second half of the pathway might be important for acetyl-CoA assimilation into succinyl-CoA. Interestingly, the first three reactions of this reverse sequence (acetoacetyl-CoA β-ketothiolase, 3-hydroxybutyryl-CoA dehydrogenase, and crotonyl-CoA hydratase) are identical to those in the acetyl-CoA assimilation pathway described for *Streptomyces collinus,* which converts acetyl-CoA to crotonyl-CoA (33). The latter, via the action of crotonyl-CoA reductase, is converted to butyryl-CoA, which is isomerized to isobutyryl-CoA by the action of a stand-alone ICM. Isobutyryl-CoA can be converted to succinyl-CoA. Thus, in organisms lacking enzymes in the first half of the 3-hydroxypropionate/4-hydroxybutyrate pathway, ICM may afford an alternative route for assimilation of acetyl-CoA.

It is interesting how MCM-like enzymes have evolved distinct substrate specificities by virtue of very limited changes in their active site residues. Muller and co-workers (39, 40) described a B_{12}-dependent enzyme that is involved in the pathway of degradation of fuel oxygenates. This enzyme in *Methylibium petroleiphilum* PM1 was shown to convert 2-hydroxyisobutyryl-CoA into 3-hydroxybutyryl-CoA. The remarkable feature of this enzyme is that it resembles ICM and has two subunits, IcmA and IcmB. However, in the active site of IcmA, Phe is substituted by Ile, whereas Gln is conserved (see Fig. 5 in Ref. 39). It is interesting that *M. petroleiphilum* also has a copy of the *icmF* and *mcm* genes (based on amino acid substitutions in the active site sequences). Another example of subtle alterations in substrate specificity is seen in ethylmalonyl-CoA mutase from *Rhodobacter sphaeroides* (41). This enzyme interconverts ethylmalonyl-CoA and methylsuccinyl-CoA. Like MCM, ethylmalonyl-CoA mutase is predicted to have Tyr and Arg residues in the active site. However, to utilize the larger

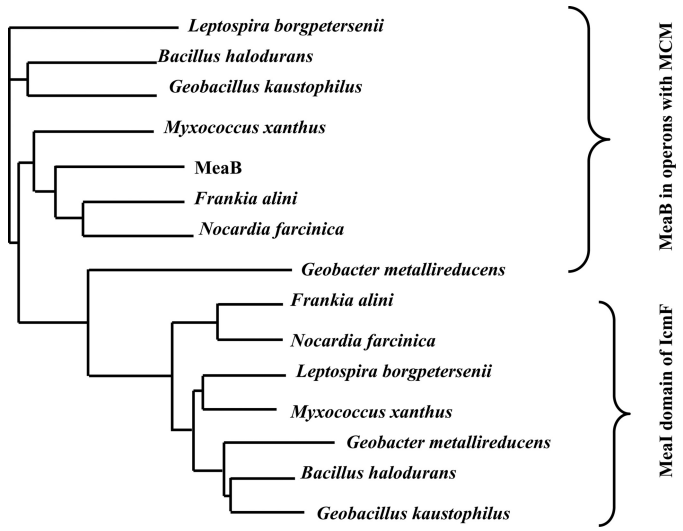

FIGURE 9. **Phylogenetic tree of MeaBs that is located in operons with MCM and MeaIs that are fused to ICM (IcmF).** MeaB-like sequences in the same operon with MCM are as follows: MeaB(AAL86727), *B. halodurans* (NP_243820), *Frankia alini* (YP_715132), *G. kaustophilus* (YP_148222), *Geobacter metallireducens* (YP_385162), *Leptospira borgpetersenii* (YP_799393), *M. xanthus* (YP_630483), and *N. farcinica* (YP_119677). MeaI sequences that are part of IcmF are as follows: *B. halodurans* (NP_244663), *F. alini* (YP_716016), *G. kaustophilus* (YP_149244), *G. metallireducens* (YP_384678), *L. borgpetersenii* (YP_801321), *M. xanthus* (YP_630482), and *N. farcinica* (YP_117245).

ethylmalonyl-CoA/methylsuccinyl-CoA substrates, it is speculated that a conserved His and Asn in MCM are substituted by Gly-255 and Pro-296, respectively, in the *R. sphaeroides* ethylmalonyl-CoA mutase (see supplemental Fig. S4 in Ref. 41). The identification of ICM- and IcmF-encoding genes in a number of bacteria and archaea should fuel studies aimed at identifying the metabolic contributions of the ICM activity in these organisms.

Acknowledgments—We thank Dr. Bruce Palfey (University of Michigan, Ann Arbor) for providing purified porcine liver butyryl-CoA dehydrogenase and for help in the developing of coupled assay and Dr. Donald Becker (University of Nebraska, Lincoln) for providing the M. elsdenii BDH expression construct.

REFERENCES

1. Zerbe-Burkhardt, K., Ratnatilleke, A., Philippon, N., Birch, A., Leiser, A., Vrijbloed, J. W., Hess, D., Hunziker, P., and Robinson, J. A. (1998) *J. Biol. Chem.* **273,** 6508–6517
2. Ratnatilleke, A., Vrijbloed, J. W., and Robinson, J. A. (1999) *J. Biol. Chem.* **274,** 31679–31685
3. Vrijbloed, J. W., Zerbe-Burkhardt, K., Ratnatilleke, A., Grubelnik-Leiser, A., and Robinson, J. A. (1999) *J. Bacteriol.* **181,** 5600–5605
4. Banerjee, R., and Chowdhury, S. (1999) in *Methylmalonyl-CoA Mutase* (Banerjee, R., ed) pp. 707–730, John Wiley & Sons, Inc., New York
5. Drennan, C. L., Huang, S., Drummond, J. T., Matthews, R. G., and Lidwig, M. L. (1994) *Science* **266,** 1669–1674
6. Holloway, D. E., and Marsh, E. N. (1994) *J. Biol. Chem.* **269,** 20425–20430
7. Banerjee, R. (2003) *Chem. Rev.* **103,** 2083–2094
8. Dobson, C. M., Wai, T., Leclerc, D., Wilson, A., Wu, X., Doré, C., Hudson, T., Rosenblatt, D. S., and Gravel, R. A. (2002) *Proc. Natl. Acad. Sci. U.S.A.* **99,** 15554–15559
9. Hubbard, P. A., Padovani, D., Labunska, T., Mahlstedt, S. A., Banerjee, R., and Drennan, C. L. (2007) *J. Biol. Chem.* **282,** 31308–31316
10. Leipe, D. D., Wolf, Y. I., Koonin, E. V., and Aravind, L. (2002) *J. Mol. Biol.* **317,** 41–72
11. Gasper, R., Scrima, A., and Wittinghofer, A. (2006) *J. Biol. Chem.* **281,** 27492–27502
12. Zambelli, B., Musiani, F., Savini, M., Tucker, P., and Ciurli, S. (2007) *Biochemistry* **46,** 3171–3182
13. Jeon, W. B., Cheng, J., and Ludden, P. W. (2001) *J. Biol. Chem.* **276,** 38602–38609
14. Padovani, D., and Banerjee, R. (2006) *Biochemistry* **45,** 9300–9306
15. Padovani, D., Labunska, T., and Banerjee, R. (2006) *J. Biol. Chem.* **281,** 17838–17844
16. Korotkova, N., and Lidstrom, M. E. (2004) *J. Biol. Chem.* **279,** 13652–13658
17. Berg, I. A., Kockelkorn, D., Buckel, W., and Fuchs, G. (2007) *Science* **318,** 1782–1786
18. Takami, H., Takaki, Y., Chee, G. J., Nishi, S., Shimamura, S., Suzuki, H., Matsui, S., and Uchiyama, I. (2004) *Nucleic Acids Res.* **32,** 6292–6303
19. Ishikawa, J., Yamashita, A., Mikami, Y., Hoshino, Y., Kurita, H., Hotta, K., Shiba, T., and Hattori, M. (2004) *Proc. Natl. Acad. Sci. U.S.A.* **101,** 14925–14930
20. Becker, D. F., Fuchs, J. A., Banfield, D. K., Funk, W. D., MacGillivray, R. T., and Stankovich, M. T. (1993) *Biochemistry* **32,** 10736–10742
21. Taoka, S., Padmakumar, R., Lai, M. T., Liu, H. W., and Banerjee, R. (1994) *J. Biol. Chem.* **269,** 31630–31634
22. Birch, A., Leiser, A., and Robinson, J. A. (1993) *J. Bacteriol.* **175,** 3511–3519
23. Lehman, T. C., Hale, D. E., Bhala, A., and Thorpe, C. (1990) *Anal. Biochem.* **186,** 280–284
24. Snel, B., Lehmann, G., Bork, P., and Huynen, M. A. (2000) *Nucleic Acids Res.* **28,** 3442–3444
25. Alm, E. J., Huang, K. H., Price, M. N., Koche, R. P., Keller, K., Dubchak, I. L., and Arkin, A. P. (2005) *Genome Res.* **15,** 1015–1022
26. Pandit, S. B., and Srinivasan, N. (2003) *Proteins* **52,** 585–597
27. Zerbe-Burkhardt, K., Ratnatilleke, A., Vrijbloed, J. W., and Robinson, J. A. (1998) in *Chemistry and Biochemistry of B_{12}* (Banerjee, R., ed) pp. 859–870, John Wiley & Sons, Inc., New York
28. Montoro-García, S., Martínez-Martínez, I., Navarro-Fernández, J., Takami, H., García-Carmona, F., and Sánchez-Ferrer, A. (2009) *J. Bacteriol.* **191,** 3076–3085
29. Mansoorabadi, S. O., Padmakumar, R., Fazliddinova, N., Vlasie, M., Banerjee, R., and Reed, G. H. (2005) *Biochemistry* **44,** 3153–3158
30. Enright, A. J., Iliopoulos, I., Kyrpides, N. C., and Ouzounis, C. A. (1999) *Nature* **402,** 86–90
31. Snel, B., Bork, P., and Huynen, M. (2000) *Trends Genet.* **16,** 9–11
32. Vlasie, M. D., and Banerjee, R. (2004) *Biochemistry* **43,** 8410–8417
33. Akopiants, K., Florova, G., Li, C., and Reynolds, K. A. (2006) *J. Ind. Microbiol. Biotechnol.* **33,** 141–150
34. Asanuma, N., Ishiwata, M., Yoshii, T., Kikuchi, M., Nishina, Y., and Hino, T. (2005) *Curr. Microbiol.* **51,** 91–94
35. Miller, T. L., and Jenesel, S. E. (1979) *J. Bacteriol.* **138,** 99–104
36. Gerth, K., Jansen, R., Reifenstahl, G., Höfle, G., Irschik, H., Kunze, B., Reichenbach, H., and Thierbach, G. (1983) *J. Antibiot.* **36,** 1150–1156
37. Bode, H. B., Meiser, P., Klefisch, T., Cortina, N. S., Krug, D., Göhring, A., Schwär, G., Mahmud, T., Elnakady, Y. A., and Müller, R. (2007) *ChemBioChem* **8,** 2139–2144
38. Alber, B. E., Kung, J. W., and Fuchs, G. (2008) *J. Bacteriol.* **190,** 1383–1389
39. Rohwerder, T., Breuer, U., Benndorf, D., Lechner, U., and Müller, R. H. (2006) *Appl. Environ. Microbiol.* **72,** 4128–4135
40. Müller, R. H., Rohwerder, T., and Harms, H. (2008) *Microbiology* **154,** 1414–1421
41. Erb, T. J., Rétey, J., Fuchs, G., and Alber, B. E. (2008) *J. Biol. Chem.* **283,** 32283–32293